AIP Journal of Applied Physics

First-principles study on the magnetic properties in Mg doped BiFeO3 with and without oxygen vacancies

Ruipeng Yang, Sixian Lin, Xiaogong Fang, Xingsen Gao, Min Zeng, and Junming Liu

Citation: Journal of Applied Physics **114**, 233912 (2013); doi: 10.1063/1.4850975
View online: http://dx.doi.org/10.1063/1.4850975
View Table of Contents: http://scitation.aip.org/content/aip/journal/jap/114/23?ver=pdfcov
Published by the AIP Publishing

First-principles study on the magnetic properties in Mg doped $BiFeO_3$ with and without oxygen vacancies

Ruipeng Yang,[1] Sixian Lin,[1] Xiaogong Fang,[1] Xingsen Gao,[1] Min Zeng,[1,a)] and Junming Liu[2,b)]
[1]*Institute for Advanced Materials, South China Normal University, Guangzhou 510006, China*
[2]*Laboratory of Solid State Microstructures, Nanjing University, Nanjing 210093, China*

(Received 1 October 2013; accepted 4 December 2013; published online 19 December 2013)

The magnetic properties of Mg-doped $BiFeO_3$ (BFO) with and without oxygen vacancies are studied through first-principles calculations. The Mg-doping prefers to occupy the ferromagnetic planes and produces an obvious improved magnetization, and the magnetization is linearly enhanced with increasing Mg-doped content, which is consistent with the trend reported in experiment. However, our calculated result is significantly larger than the experimental one, and the reason is revealed that the relative energy differences of various spin-ordering configurations are small. Furthermore, oxygen vacancy in Mg-doped BFO can further enhance the magnetization, while keeping the insulating band gap character. The calculated results imply that the oxygen vacancy in Mg-doped BFO would be an effective way to improve the multiferroicity of BFO. [http://dx.doi.org/10.1063/1.4850975]

I. INTRODUCTION

Multiferroics with magnetoelectric properties have recently become the focus of intensive research due to coexistence of magnetic and electric ordering parameters, which is of interest for novel exciting applications like magnetic field sensors, tunable microwave devices, multiple state memory elements, and spintronic devices.[1–3] $BiFeO_3$ (BFO) is the known multiferroic oxide, which simultaneously processes antiferromagnetic, ferroelectric, and ferroelastic properties at room temperature as it has a ferroelectric Curie temperature of ~1100 K and a Neel temperature of ~640 K.[4] The large spontaneous polarization $P \sim 100\,\mu C/cm^2$, reported in thin film and single crystal forms, mainly originates from the Bi atom off-center distortion.[5–7] However, its magnetism is very weak in the macroscopic size as it has an incommensurate sinusoidal spin arrangement with wavelength of 62 nm.[8]

Although BFO exhibits a large ferroelectric polarization, the magnetoelectric coupling effect is very small owing to its antiferromagnetic spin ordering, which further inhibits its extensive applications. In the past decades, people have tried many methods to improve the magnetism, in turn, magnetoelectric coupling effect.[9–18] Among them, the substitution of A- and/or B-sites by other elements in BFO is extensively adopted as when these sites are occupied by different magnetic/non-magnetic ions, the space-modulated antiferromagnetic state would be broken owing to the structural distortion so that the magnetism and even magnetoelectric coupling effect are enhanced. For examples, the enhanced ferromagnetism has been revealed in BFO ceramics with the partial substitution of Fe^{3+} ions by the Ca^{2+}, Mg^{2+}, Ti^{4+}, Mn^{4+}.[9–13] The enhanced multiferroic properties of BFO ceramics have been reported in the partial substitution of Bi^{3+} ions by the rare earth elements such as Nd^{4+}, La^{3+}, Dy^{3+}.[14–19] In addition, intrinsic lattice defects in BFO have been proposed to a possible source of magnetization. For instance, Ederer and Spaldin[19] reported a slightly improved magnetization in BFO induced by oxygen vacancies in theory. Among those systems reported, the addition of Mg^{2+} ions to BFO was believed to maintain the structural stability as Mg^{2+} has a similar ion size with Fe^{3+}. In particular, it can suppress the antiferromagnetic spin ordering and introduce some oxygen vacancies through nonstoichiometric compositions. Wu *et al.*[11] reported the enhanced magnetism in Mg-doped BFO ceramics and explained the reasons as the creation of unbalanced Fe^{3+} spins and long range coupling among them mediated by localized charge carriers related to oxygen vacancies. However, the electronic mechanism for the enhanced magnetism in Mg-doped BFO is lack. Thus, a detailed investigation on the magnetic properties of Mg-doped BFO is needed. We hope the mechanism can supply the guidance for further useful studies.

In this paper, we performed first-principles calculations on the magnetic properties of Mg-doped BFO with the consideration of doped contents, charge states, and oxygen vacancies. The calculated results were compared with the experimental data. It was found that Mg-doping induces an obvious improvement in the magnetization, which is linearly enhanced with the increase of Mg-doped content. The trend is consistent with the one in experiment. However, the experimental results are significantly smaller than the theoretical values. The reason can be attributed to the very small relative energies differences of various spin-orderings configurations so that the Mg dopants in BFO do not have the energetic preference to form a special spin ordering structure. Furthermore, we found that the oxygen vacancy in Mg-doped BFO can further enhance the magnetization and maintain the insulating band gap character. Our theoretical results imply that the multiferroic behavior in BFO would be improved through combining Mg-doping and oxygen vacancies.

a)E-mail: zengmin@scnu.edu.cn
b)E-mail: liujm@nju.edu.cn

II. COMPUTATION METHOD

We selected the projector augmented wave (PAW) method to perform our first-principles calculations with the local spin-density approximation plus the on-site repulsion (LSDA + U),[20,21] implemented in the Vienna *ab initio* simulation package (VASP).[22,23] We used $U_{\text{eff}} = 3$ eV on Fe $3d$ states as other studies before for a better description of the localized transition.[24] The basis was treated with Bi $5d^{10}6s^26p^3$, Fe $3p^63d^64s^2$, O $2s^22p^4$, and Mg $2p^63s^2$. We used the energy cutoff of 400 eV for the plane wave expansion of the PAW, and the tetrahedron method for the Brillouin zone integrations. The convergence threshold for self-consistent iteration is set at 10^{-6} eV. In order to model BFO crystal structures with doping and vacancy configurations, we built a $2 \times 2 \times 2$ periodic supercell (80 atoms) based on the optimized primitive cell, see Figure 1. In practical calculations, antiferromagnetic (AFM) spin orderings are assumed for perfect BFO as it has a nearly G-type AFM configuration observed in experiment. Doping and vacancy structures can be created by replacing Fe atom by Mg atom and removing oxygen atom, respectively. All calculated structures were relaxed in a $3 \times 3 \times 3$ Monkhorst Pack grid of k points until all components of the residual forces are smaller than 1 meV/Å.

III. RESULTS AND DISCUSSION

To understand the origin of the magnetization in Mg doped BFO, we first studied one-Mg-atom-doped model, which is constructed by replacing one Fe atom at the 0 site using one Mg atom in the supercell, see Fig. 1 (the Mg-doping density is 6.25%). The calculated total density of states (TDOS) of Mg-doped BFO is shown in Fig. 2 along with the perfect BFO as a comparison. For perfect BFO, our calculated band gap is about 2.35 eV, which is in good agreement with the previous experimental data (2.5 eV)[25] and the theoretical values (2.2 ~ 2.8 eV).[24,26] The significant differences in TDOS are presented in the Mg-doped BFO due to the broken symmetry of original *R3c* structure, see Fig. 2(b). It is found that some electronic states are excited into the band gap, see the top of valence band in the minority and the bottom of conduction band in the majority, means that

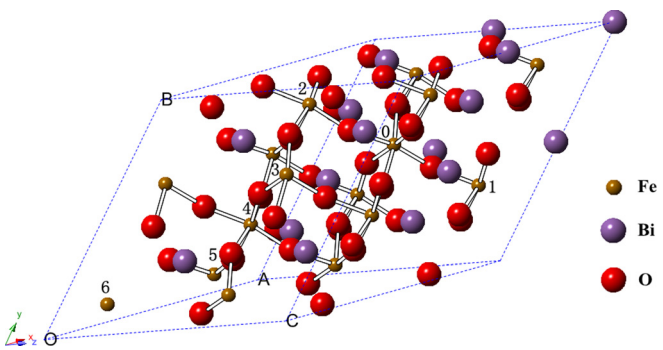

FIG. 1. The $2 \times 2 \times 2$ supercell of rhombohedral BFO containing 16 Bi (white), 16 Fe (blue), and 48 O (red) atoms with the labeled Mg-doped atomic sites. Here, two Fe atoms at different sites are replaced by two Mg atoms, which gives six distinct pairs of Mg atoms, such as (0, 1), (0, 2), (0, 3,), (0, 4), (0, 5), (0, 6), respectively.

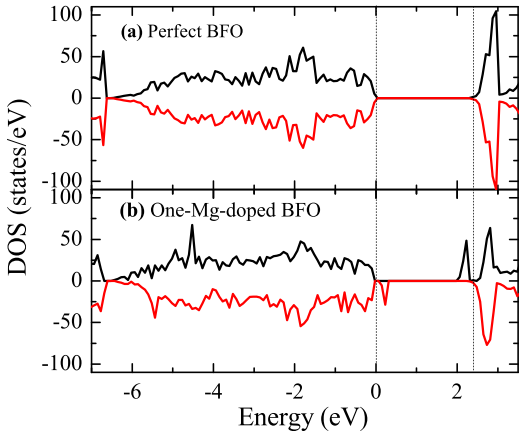

FIG. 2. The total electronic density of states for (a) the perfect and (b) one-Mg-doped BFO.

Mg-doped BFO has a typical p-type conducting character. It is noticed that the Mg-doped BFO generates a net magnetic moment of about 4.28 μ_B compared with the no magnetic moment in the perfect BFO. Actually, the magnetic moment originates from the suppression of the spatially modulated AFM spin ordering. It is well-known that the magnetization in BFO mainly originates from the magnetic moment Fe atoms. Our calculated results show that the magnetic moment of Fe atom in the perfect BFO structure is about $\pm 4.16\,\mu_B$. It is the Fe^{3+}-O-Fe^{3+}AFM spin ordering that leads to a no net magnetic moment in perfect BFO. However, the AFM spin ordering network in one-Mg-atom-doped BFO is disrupted so that the spin ordering is changed from AFM to ferrimagnetism. The induced magnetic moment of 4.28 μ_B is almost equal to the individual local magnetic moment of Fe atom (4.16 μ_B).

Notice that the substitution in this one-Mg-atom-doped model is nonsymmetrical, i.e., a ferrimagnetism spin ordering is established artificially without considering the randomly or nonsymmetrical distribution of the Mg dopants. To clarify the type of spin ordering distributions between the two Mg dopants, six different spin ordering configurations are modeled using the 80-atom 2 × 2 × 2 supercell, which are constructed by replacing two Fe atoms using two Mg atoms at positions (0, 1), (0, 2), (0, 3), (0, 4), (0, 5), and (0, 6), respectively, as shown in Fig. 1 (the Mg-doping density is 12.5%). For convenience, we use (i, j) to denote the structure in which the Fe atoms at the positions of (i, j) are replaced by Mg atoms. During the calculation, the spin orientation of other Fe atoms is the same with the perfect BFO. In Table I, we summarized the calculated results for Mg-doped BFO. For each structure, the Mg-Mg distance $d_{\text{Mg-Mg}}$, relative energy ΔE, and total magnetic moment are listed. For the (i, j) configuration, the relative energy is defined as the energy difference between the energy of the (0, j) and the total energy of the (0, 1) structure, i.e., $\Delta E = E(\text{i, j}) - E(0, 1)$. Clearly, the relative energy ΔE of (0, 6) structure is the lowest among six configurations, means that it is the most stable structure from the energy viewpoint. Correspondingly, the magnetic moment in (0, 6) structure is about 8.3 μ_B, which is equivalent to the twice of one-Mg-atom-doped BFO. However, we find that two Mg-dopants lying in two

TABLE I. Calculated results for Mg-doped BFO: the optimized Mg…Mg distance ($d_{Mg\text{-}Mg}$) (Å), the relative energies ΔE (eV), and total magnetic moment (M) (μ_B).

(i, j)	(0, 1)	(0, 2)	(0, 3)	(0, 4)	(0, 5)	(0, 6)
$d_{Mg\text{-}Mg}$	3.86	4.13	5.44	4.36	9.40	13.28
ΔE	0	0.0056	−0.0504	0.0162	−0.0644	−0.0880
M	0.003	−0.019	−8.910	−0.423	−8.306	−8.333

antiferromagnetically aligned planes produce no net magnetic moment, see the (0, 1), (0, 2), and (0, 4) structures.

It is also worthy noticing that the charge in this two-Mg-atom-doped model is non-neutral. To clarify the effect of charge on the magnetic property, we took into account with the consideration of possible charge states of q = 0, −1, and −2 in (0, 6) structure. It is found that the calculated TDOS and magnetic moments are almost same among various charge states, indicating that the magnetism could be stabilized at charge states of 1− and 2−. However, the electronic structure in the two-Mg-atom-doped model, see Figure 3(a) for the 2^- charge state as an example, is significantly different from that of the one-Mg-atom-doped BFO. It is found that the two-Mg-atom-doped structure has half-metallic characteristic with the spin-down DOS is metallic at Fermi level, while the spin-up DOS is insulating with a large band gap. In addition, the charge-neural state in the two-Mg-atom-doped model can be created by introducing one oxygen vacancy. In our calculation, the oxygen vacancy is created by removing the oxygen atom between two Mg atoms without considering the randomness and the calculated TDOS is presented in Figure 3(b). The interesting feature is that the electronic state in Fermi level is absent, means that oxygen vacancy inhibits Mg-doped BFO to form half-metal band gap character. Furthermore, the magnetic moment is further enhanced, and the value is up to 10 μ_B. It should be noted that there do not have such apparent increase if oxygen vacancy is not in this specific. Thus, it can be expected that Mg-doped BFO with this special charge-neural oxygen state has an improved multiferroicity due to the large magnetization and good insulating band gap property (i.e., its ferroelectric polarization would not be degraded).

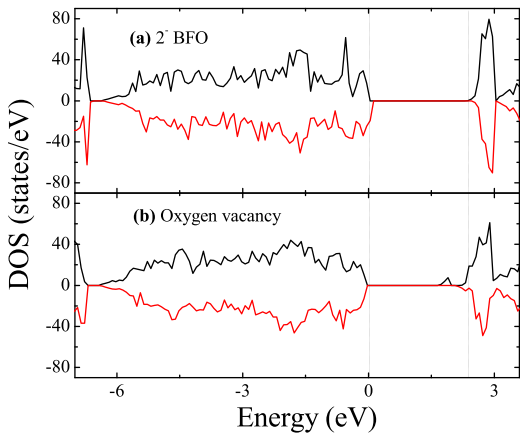

FIG. 3. The total electronic density of states for (a) the 2^- charge state two-Mg-atom-doped BFO and (b) the charge-neural state two-Mg-atom-doped BFO created by introducing one oxygen vacancy.

In order to further investigate the origin of magnetism in two-Mg-doped BFO, the spin density distributions are studied, and the results are shown in Figure 4 for perfect and two-Mg-atoms-doped BFO in $(\bar{1}10)$ projected plane. The two axes are [110] and [001], respectively. The vertical axis is [111] direction. It is clearly observed that the spin moment is mainly originated from Fe atoms. Meanwhile, O atoms also generate weak local spin moments due to the strong hybridizations between Fe and O atoms, see Fig. 4(a). In Mg-doped system, the Mg sites (see the dotted cycles in Fig. 4(b)), corresponding to the center of positive charges induces Coulomb repulse and attraction with the neighbor's Fe and O atoms, respectively. Consequently, a distortion is observed in the FeO_6 octahedrons near the Mg sites which make a set of three Fe-O bonds to be shorted and another set of three Fe-O bands to be elongated so that the spin moments are enhanced in the one end of shorter Fe-O bonds and disappeared in the another end of longer Fe-O bonds, see the straight cycles. In addition, oxygen vacancy in two Mg-doped BFO further enhances the Fe-O hybridization near vacancy and generates an enhanced magnetism, and the spin density distribution is similar to the one in Fig. 4(b).

Finally, a comparison of the magnetic moment between theoretical calculation and experimental results is presented in Figure 5. It is found that the theoretical results (1 μ_B per unit cell corresponds to ∼150 emu/g) have the same tendency as experiment,[11] with increasing Mg-doped content, both of them increase linearly. However, it is worthy noticing that the experimental value is much smaller than the theoretical one (the result calculated in (0, 6) structure, see Table I). The difference can be explained that the six configurations have very close energies with one and another, and the difference between the lowest and highest ones is only 0.088 eV, suggesting that real materials certainly would be a mixture of the six configurations. In contrast to this small energy difference, the magnetic moments of these configurations show a difference as big as ∼8.9 emu, and in particular, the configurations (0, 1), (0, 2), and (0, 4) have zero effect moment. Therefore, one has reason to claim that the measured moment should be much smaller than the highest moment predicted from our first-principles calculation.

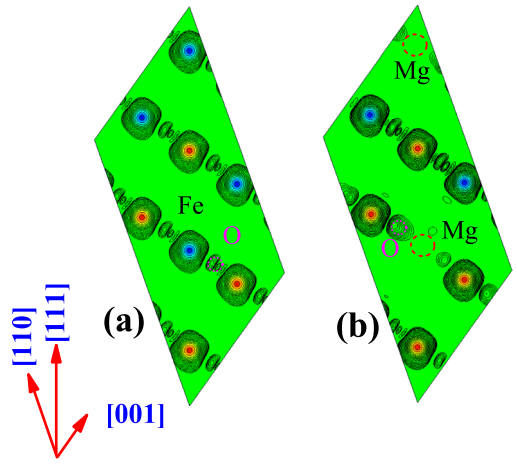

FIG. 4. The spin density distributions of (a) perfect BFO, (b) two-Mg-doped BFO in the $(\bar{1}10)$ plane. The Mg and O sites are labeled by dotted and straight circles, respectively.

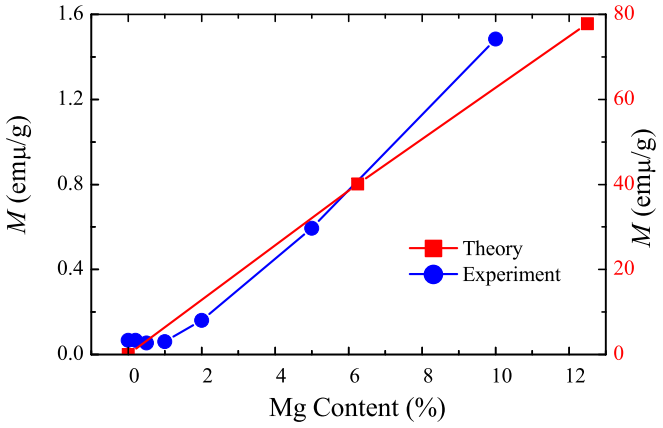

FIG. 5. The magnetic moment comparison among different Mg-doping concentrations. The red and the blue lines represent the magnetic results in theoretical calculation and experiment, respectively.

It is well known that Mg^{2+} has a similar ion size with Fe^{3+}, the replacement of Fe^{3+} by Mg^{2+} ions would retain the structure stability. On the other hand, replacing the magnetic ion with the nonmagnetic one would induce the imbalance of magnetic moment, which is the possible source of magnetism, see Fig. 4. However, the large magnetization is few reported in experiment, which is attributed to the small energy difference in Mg-doped BFO with the ferromagnetism and AFM spin ordering configurations. In particular, the half metallic properties are also presented in Mg-doped BFO, which can degrade ferroelectric polarization. In contrast, oxygen vacancy introduced in Mg-doped BFO can further enhance its magnetism and keep the insulating band gap character. Experimentally, a ferroelectric polarization is not reported, the reason may be that some impurity phases could be produced easily during in traditional fabrication process.[11] Thus, we hope that our theoretical results predict will inspire further experimental research in Mg-doped BFO with oxygen vacancies for multiferroics.

IV. CONCLUSIONS

In summary, the first-principles calculated results showed that Mg-substitution of Fe would induce the obvious increase of magnetic moment, which is linearly varied as the Mg content increases. The results were very different from the experiment those from the numerical view, but they had the same trend, and the reasons were caused by the small energy differences between spin-ordering configurations. In addition, the change of electrovalence induced by Mg^{2+} replacing Fe^{3+} would not seriously affect the magnetic moment. Finally, the multiferroic behaviors would be improved in Mg-doped BFO through introducing some oxygen vacancies because the insulating property (the widen band gap) is not degraded when the magnetism is enhanced greatly. The theoretical results imply that the oxygen vacancy in Mg-doped BFO would be an effective way to improve the multiferroicity of BFO.

ACKNOWLEDGMENTS

The authors gratefully acknowledge financial support from the National Science Foundation of China (Grant Nos. 51101063, 51272078, and 51332007), and the Natural Science Foundation of Guangdong Province of China (No. S2011040003205).

[1]R. Ramesh and N. A. Spaldin, Nature Mater. **6**, 21 (2007).
[2]K. F. Wang, J.-M. Liu, and Z. F. Ren, Adv. Phys. **58**, 321 (2009).
[3]S. W. Cheong and M. Mostovoy, Nature Mater. **6**, 13 (2007).
[4]G. A. SmolenskiK and I. E. Chupis, Sov. Phys. Usp. **25**, 475 (1982).
[5]J. Wang, J. Neaton, H. Zheng, V. Nagarajan, S. Ogale, B. Liu, D. Viehland, V. Vaithyanathan, D. Schlom, and U. Waghmare, Science **299**, 1719 (2003).
[6]J. B. Neaton, C. Ederer, U. V. Waghmare, N. A. Spaldin, and K. M. Rabe, Phys. Rev. B **71**, 014113 (2005).
[7]G. Catalan and J. F. Scott, Adv. Mater. **21**, 2463 (2009).
[8]R. E. Cohen, Nature **358**, 136 (1992).
[9]B. Ramachandran, A. Dixit, R. Naik, G. Lawes, and M. S. Ramachandra Rao, J. Appl. Phys. **111**, 023910 (2012).
[10]Y. H. Gu, Y. Wang, F. Chen, H. L. W. Chan, and W. P. Chen, J. Appl. Phys. **108**, 094112 (2010).
[11]H. Wu, Y. Lin, J. Gong, F. Zhang, M. Zeng, M. Qin, Z. Zhang, Q. Ru, Z. Liu, and X. Gao, J. Phys. D: Appl. Phys. **46**, 145001 (2013).
[12]L. Y. Zou, R. P. Yang, Y. B. Lin, M. H. Qin, X. S. Gao, M. Zeng, and J.-M. Liu, J. Appl. Phys. **114**, 034105 (2013).
[13]V. A. Khomchenko, D. V. Karpinsky, L. C. J. Pereira, A. L. Kholkin, and J. A. Paixao, J. Appl. Phys. **113**, 214112 (2013).
[14]S. T. Zhang, Y. Zhang, M. H. Lu, C. L. Du, Y. F. Chen, Z. G. Liu, Y. Y. Zhu, N. B. Ming, and X. Q. Pan, Appl. Phys. Lett. **88**, 162901 (2006).
[15]G. L. Yuan, S. W. Or, J. M. Liu, and Z. G. Liu, Appl. Phys. Lett. **89**, 052905 (2006).
[16]F. Z. Qian, J. S. Jiang, S. Z. Guo, D. M. Jiang, and W. G. Zhang, J. Appl. Phys. **106**, 084312 (2009).
[17]S. K. Srivastav, N. S. Gajbhiye, and A. Banerjee, J. Appl. Phys. **113**, 203917 (2013).
[18]L. H. Yin, J. Yang, B. C. Zhao, Y. Liu, S. G. Tan, X. W. Tang, J. M. Dai, W. H. Song, and Y. P. Sun, J. Appl. Phys. **113**, 214104 (2013).
[19]C. Ederer and N. A. Spaldin, Phys. Rev. B **71**, 224103 (2005).
[20]P. E. Blöchl, Phys. Rev. B **50**, 17953 (1994).
[21]V. I. Anisimov, F. Aryasetiawan, and A. I. Lichtenstein, J. Phys.: Condens. Matter **9**, 767 (1997).
[22]G. Kresse and J. Hafner, Phys. Rev. B **47**, 558 (1993).
[23]G. Kresse and J. Furthmuller, Phys. Rev. B **54**, 11169 (1996).
[24]T. R. Paudel, S. S. Jaswal, and E. Y. Tsymbal, Phys. Rev. B **85**, 104409 (2012).
[25]J. F. Ihlefeld, N. J. Podraza, Z. K. Liu, R. C. Rai, X. Xu, T. Heeg, Y. B. Chen, J. Li, R. W. Collins, J. L. Musfeldt, X. Q. Pan, J. Schubert, R. Ramesh, and D. G. Schlom, Appl. Phys. Lett. **92**, 142908 (2008).
[26]S. J. Clark and J. Robertson, Appl. Phys. Lett. **90**, 132903 (2007).